Electronic Supplementary Material (ESI) for Nanoscale.

Multiscale Modelling Reveals Higher Charge Transport Efficiencies of DNA Relative to RNA Independent of Mechanism: Supporting Information

Abhishek Aggarwal,[1] Saientan Bag,[1] Ravindra Venkatramani,[2] Manish Jain,[1] and Prabal K. Maiti[1,*]
[1] *Center for Condensed Matter Theory, Department of Physics,*
Indian Institute of Science, Bangalore-560012, India
[2] *Department of Chemical Sciences, Tata Institute of Fundamental Research, Colaba, Mumbai-400005, India*

HOLE CURRENT FOR DIFFERENT 12 BP SEQEUNCES OF DSDNA AND DSRNA

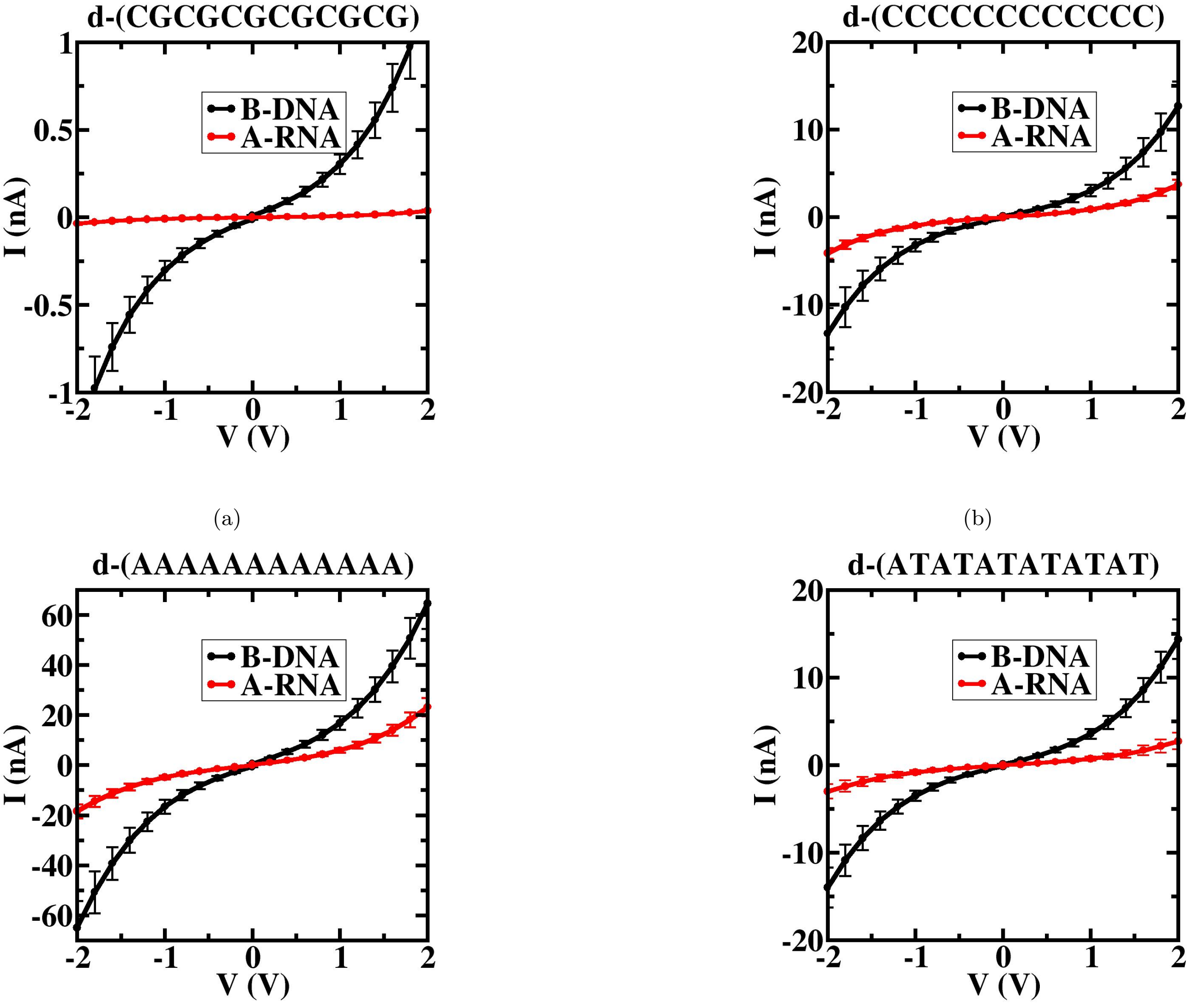

(a)

(b)

(c)

(d)

FIG. S1: Hole current for (a) $d-(CG)_6$ (b) $d-(CC)_6$ (c) $d-(AA)_6$ (d) $d-(AT)_6$ sequences of dsDNA and dsRNA using hopping mechanism. For each sequence dsDNA conducts better than dsRNA in incoherent regime.

Hole current for different sequences of dsDNA and dsRNA using hopping mechanism are shown in fig. S1. For each sequence, dsDNA conducts better than dsRNA in incoherent regime.

ELECTRONIC CURRENT FOR DIFFERENT 12 BP SEQEUNCES OF DSDNA AND DSRNA

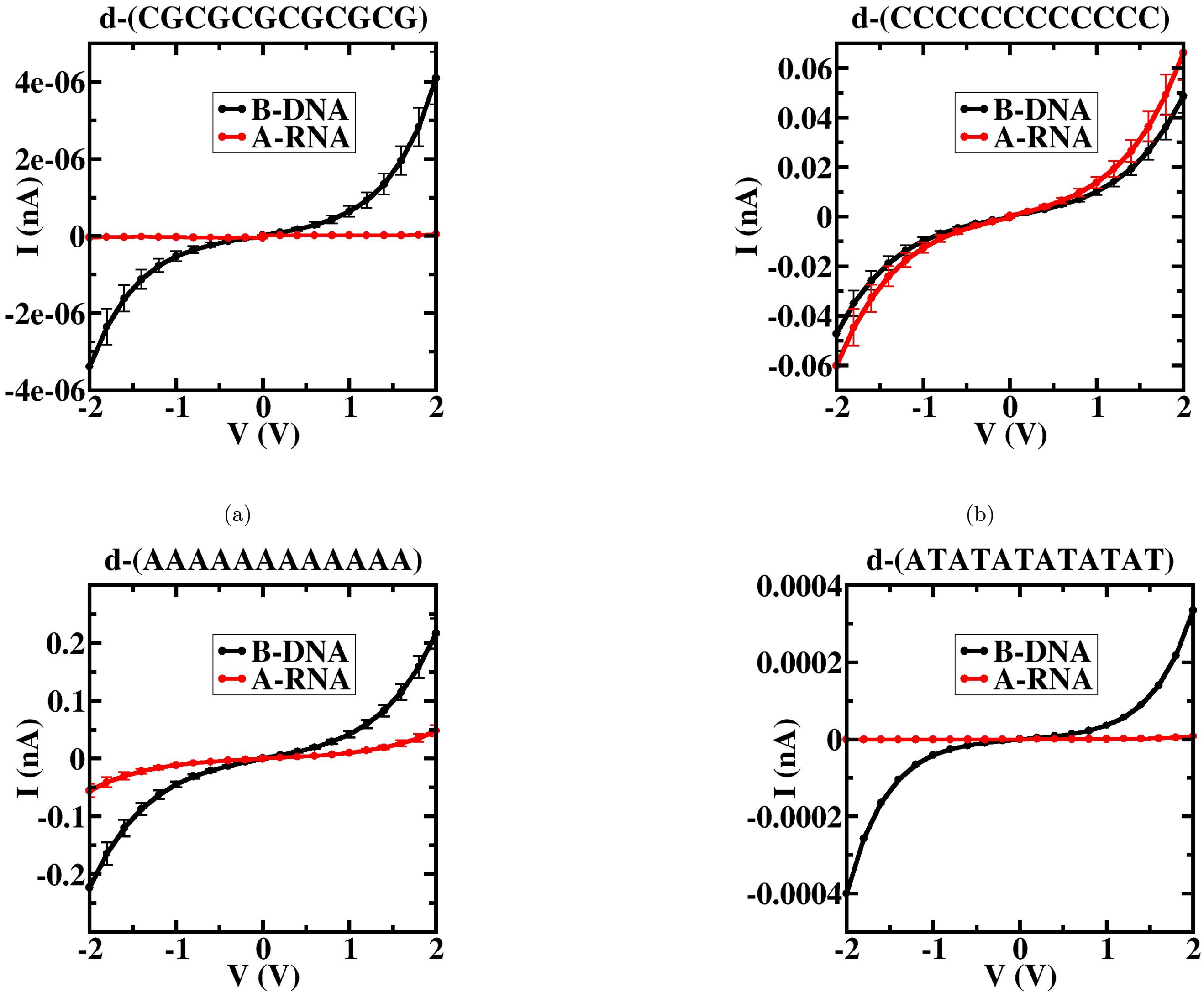

(a)

(b)

(c)

(d)

FIG. S2: Electronic current for (a) $d-(CG)_6$ (b) $d-(CC)_6$ (c) $d-(AA)_6$ (d) $d-(AT)_6$ sequences of dsDNA and dsRNA using hopping mechanism. For each sequence dsDNA conducts better than dsRNA in incoherent regime.

Electronic current for different sequences of dsDNA and dsRNA using hopping mechanism are shown in fig. S2. Although, the electronic current is lower in magnitude than hole current, dsDNA conducts better than dsRNA for each sequence in incoherent regime.

CURRENT FOR DIFFERENT 12 BP SEQEUNCES OF DSDNA AND DSRNA USING COHERENT TUNNELING MECHANISM

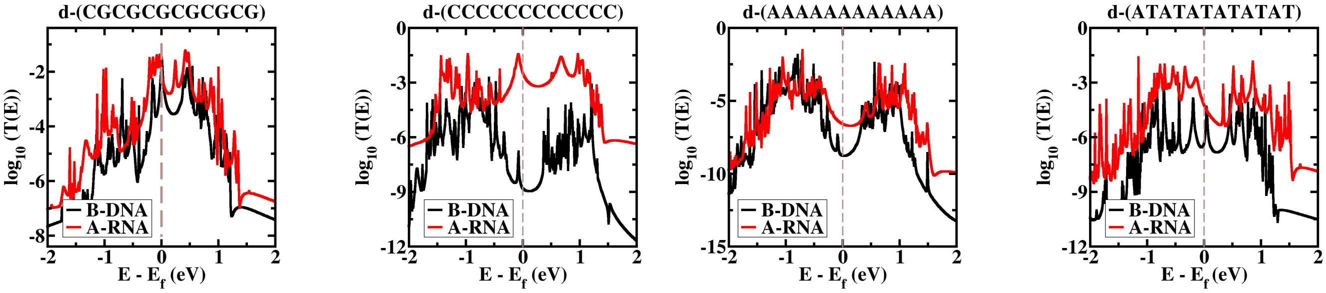

(a) (b) (c) (d)

FIG. S3: Transmission coefficient near Fermi energy region for (a) d-(CGCGCGCGCGCG) (b) d-(CCCCCCCCCCCC) (c) d-(AAAAAAAAAAAA) (d) d-(ATATATATATAT) sequences of dsDNA and dsRNA using coherent tunneling mechanism. For each sequence dsRNA has higher transmission probability than dsDNA in coherent regime.

V-I characteristics for different sequences of dsDNA and dsRNA using coherent tunneling mechanism are shown in fig. S4. For each sequence, dsRNA conducts better than dsDNA in coherent regime.

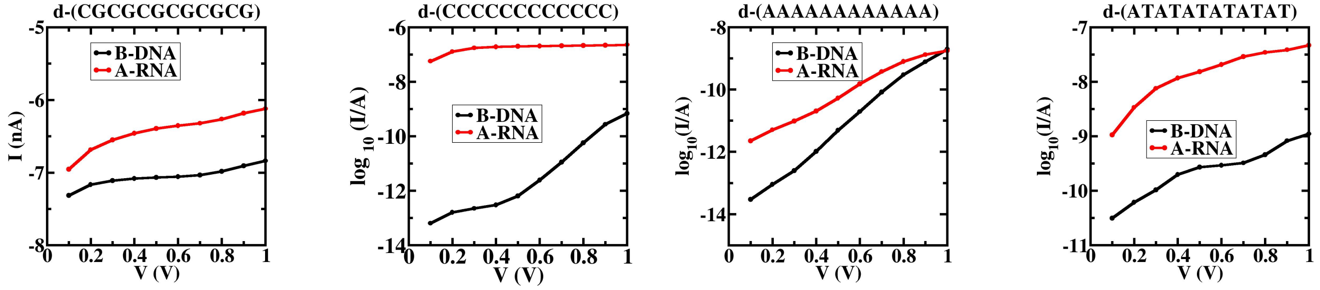

(a) (b) (c) (d)

FIG. S4: V-I characteristics for (a) d-(CGCGCGCGCGCG) (b) d-(CCCCCCCCCCCC) (c) d-(AAAAAAAAAAAA) (d) d-(ATATATATATAT) sequences of dsDNA and dsRNA using coherent tunneling mechanism. For each sequence dsRNA conducts better than in coherent tunneling regime.

EXPERIMENTAL RESULTS FOR 13 BP DSDNA AND DSRNA SEQUENCE

In order to compare the results with experiments, we also calculated the charge transport properties of 13 bp B-form dsDNA and A-form dsRNA with sequence d-(CCCGCGCGCGCCC). The charge transport properties of this sequence have been studied experimentally in Ref. [1].

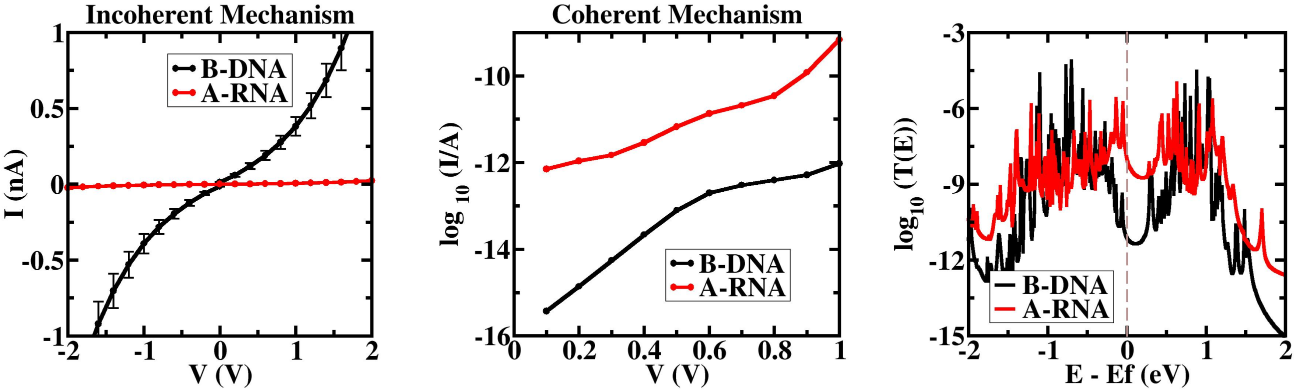

(a) (b) (c)

FIG. S5: (a) V-I characteristics curve for 13 bp (d-(CCCGCGCGCGCCC)) dsDNA vs dsRNA using hopping charge transport mechanism. The charge transport properties of this sequence have been studied experimentally in Ref. [1]. dsRNA has almost two orders of magnitude less conductance than dsDNA. (b) V-I characteristics of both 13 bp (d-(CCCGCGCGCGCCC)) dsDNA and dsRNA using coherent tunneling charge transport mechanism. (c) Variation of transmission probability vs energy for 13 bp dsDNA and dsRNA. Clearly, in tunneling mechanism, dsRNA conducts better than dsDNA by an order of magnitude which is seen experimentally as well.

DECAY CONSTANT

We have calculated the decay constant values for dsRNA in the hopping regime using the relation $G = G_0 exp^{-\beta L}$ (fig. S6a). The decay constant value of 0.16 $\mathring{A}^{-1}$ implies a weak length dependence of hole current in hopping regime. Whereas, the decay constant values of dsDNA and dsRNA in tunneling regime are 0.52 $\mathring{A}^{-1}$ and 0.74 $\mathring{A}^{-1}$ respectively indicating strong length dependence of current in coherent regime (fig. S6b). Notably, the decay constant value is higher for dsRNA relative to that of dsDNA.

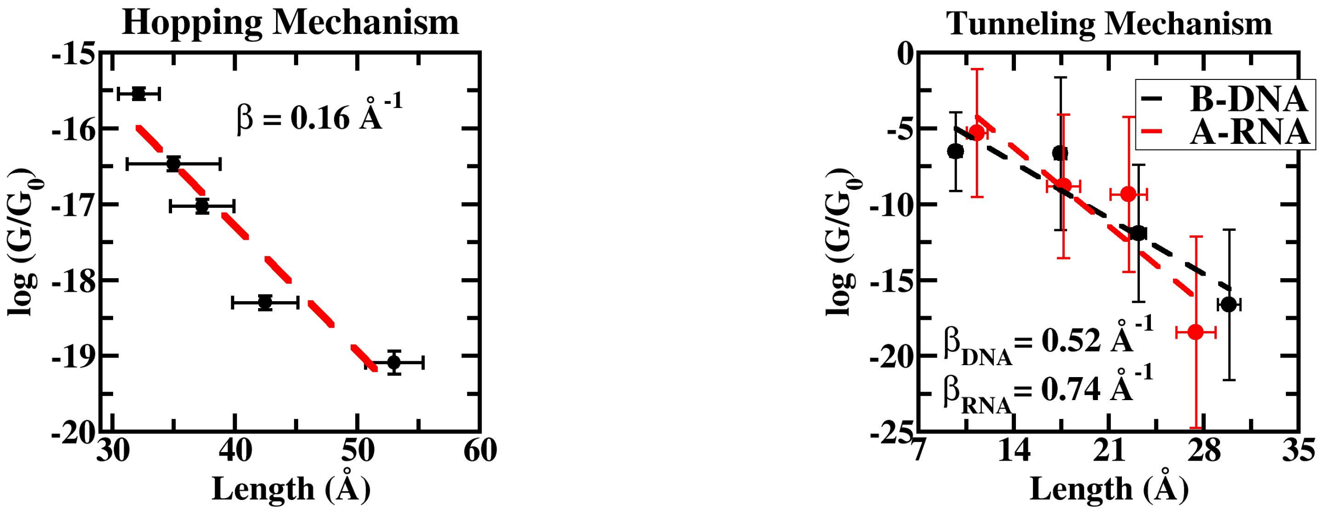

(a)

(b)

FIG. S6: (a) Graph showing the variation of conductance (ln (G/G_0)) of dsRNA in hopping regime with the length of dsRNA. The decay constant of dsRNA in hopping regime is 0.16 $\mathring{A}^{-1}$. (b) A comparison of length dependence of dsDNA and dsRNA conductance in coherent tunneling regime. The decay constant values of dsDNA and dsRNA in tunneling regime are 0.52 $\mathring{A}^{-1}$ and 0.74$\mathring{A}^{-1}$ respectively indicating strong length dependence of current in coherent regime.

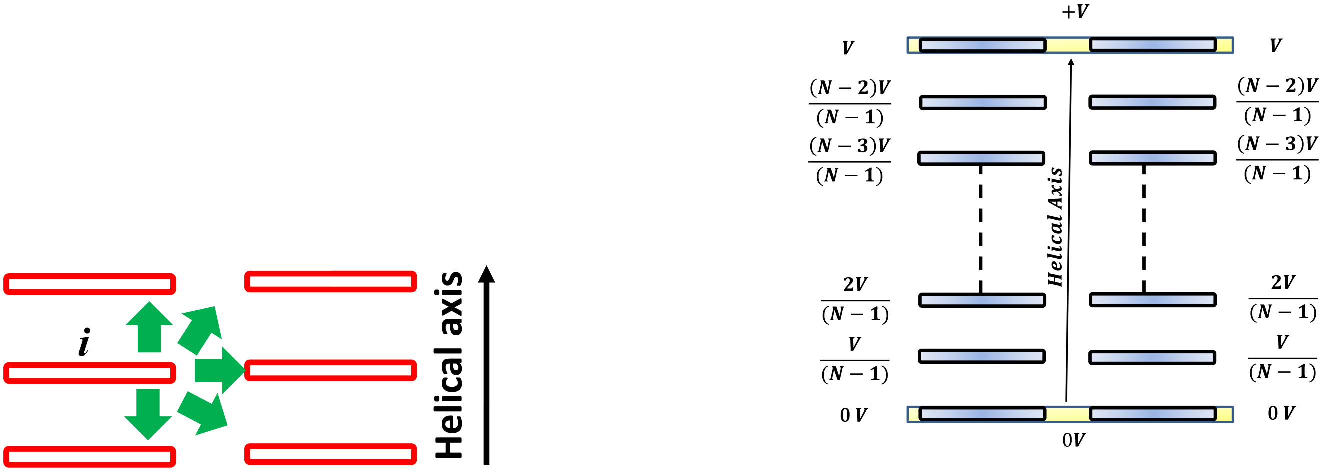

(a) (b)

FIG. S7: (a) Schematic diagram describing the available hopping sites (i.e. the nucleobases) for a charge present at a charge hopping site *i*. A charge present at a site other than terminal bases will have 5 sites to hop to. (b) Distribution of voltage along the dsDNA or dsRNA chain during charge transport calculations. Here, we have assumed that the potential is distributed uniformly along the RNA chain.

HOPPING MODEL USED FOR CHARGE TRANSPORT CALCULATIONS

We use nearest neighbour hopping model. In this model, a charge present at any hopping site other than the terminal bases has 5 available sites to hop to. These consists of 4 hopping sites from two adjacent base pairs and 5^{th} hopping site will be the complementary base of the present site. This is shown in fig S7.

Reorganization Energy and Free Energy Difference

ΔG_{ij} is the free energy difference between two sites defined as:

$$\Delta G_{ij} = \Delta G_{ij}^{int} + \Delta G_{ij}^{ext} \tag{S1}$$

ΔG_{ij}^{ext} is the contribution due to the external electric field, taken as the potential difference between the two hopping sites in our calculations. We take uniform distribution of potential between the base pairs, i.e. consecutive base pairs will have a potential difference of $(\frac{V}{(N-1)})$ (fig. S7), while bases of same pairs will have zero potential difference i.e.

$$\Delta V = \begin{cases} (\frac{V}{N-1}), \text{for consecutive bases along the helical axis of DNA or RNA along positive voltage.} \\ 0, \text{for base pairs at the same level along the helical axis.} \\ -(\frac{V}{N-1}), \text{for consecutive bases along the helical axis of DNA or RNA along negative voltage.} \end{cases} \tag{S2}$$

Whereas,

$$\Delta G_{ij}^{int} = U_i^{cC} - U_i^{nN} + U_j^{cC} - U_j^{nN} \tag{S3}$$

Where, $U_i^{nN}(U_i^{cC})$ is the internal energy of neutral (charged) base in neutral (charged) state geometry.

A comparison of reorganization energy for hole and electron transfer between different base pairs dsRNA (table SI) clearly shows that the reorganization energy for electron is always higher relative to that for hole. As the hopping rate critically depends on the reorganization energy, this difference leads to the difference in order of magnitude in hole and electron transport.

Kinetic Monte Carlo

Once the calculation of charge hopping rates between all the charge hopping sites is complete, the next task is to obtain the steady state solution of the master equation containing the probabilities of a charge hopping site to hold charge. For that, Kinetic Monte Carlo[2, 3] (KMC) method is performed. In this scheme, we assigne a unit charge to a random hopping site i. This point of time is then taken as the initial time as $t = 0$. To calculate the waiting time τ, we use the relation:

$$\tau = -\omega_i^{-1} \ln(r_1) \tag{S4}$$

where $\omega_i = \sum_{j=1}^{n} \omega_{ij}$ is the sum of all the hopping rates for the sites which are available for charge present at site i, n is the number of charge hopping sites available for charge at site i, r_1 is a uniform random number between 0 and 1 and j is just the index for the available sites for hopping. After the calculation of the waiting time, the total time is then updated as $t = t + \tau$. To decide the site to which the charge has to hop to, the j for which $\frac{\sum_j \omega_{ij}}{\omega_i}$ is largest and $\leq r_2$, is chosen where r_2 is another uniform random number between 0 and 1. The above condition ensures that the site j is chosen with probability $\frac{\omega_{ij}}{\omega}$. After this, we update the position of the charge and repeat the above process which provides the probabilities for each site. The current is then found using the following formula [4],

$$I_{bp} = -e[\sum_i (P_{b_1}\omega_{b_1 i} - P_i \omega_{i b_1}) + \sum_i (P_{b_2}\omega_{b_2 i} - P_i \omega_{i b_2})] \tag{S5}$$

Here, e is the unit electric charge, i stands for all the possible hopping sites which are in the direction of flow of current, b_1 and b_2 are the base stacks of base pair bp. Hence mean current is average over all base pairs, $I = < I_{bp} >$.

TABLE SI: Table comparing the reorganization energy for hole and electron transfer between different base pairs dsRNA

From	To	Hole (eV)	Electron (eV)
A	A	0.57	0.65
A	C	0.46	0.84
A	G	0.64	0.73
A	U	0.55	0.73
C	A	0.54	0.93
C	C	0.43	1.12
C	G	0.61	1.01
C	U	0.51	1.01
G	A	0.61	1.20
G	C	0.50	1.39
G	G	0.68	1.28
G	U	0.58	1.28
U	A	0.60	0.98
U	C	0.49	1.17
U	G	0.67	1.06
U	U	0.57	1.06

EFFECT OF EXTERNAL REORGANIZATION ENERGY ON HOPPING CHARGE TRANSPORT OF DSDNA AND DSRNA

The external reorganization energy, λ_{ij}, has two parts : inner sphere reorganization energy and outer sphere reorganization energy. The outer sphere reorganization energy is varied from 0 eV to 1 eV and the effect on the current at an applied potential bias of 1 V through dsDNA and dsRNA has been plotted in fig. S8. Clearly, dsDNA conducts better relative to dsRNA for all outersphere reorganization energy values. Hence, outersphere reorganization energy is taken as 0 in all the calculations.

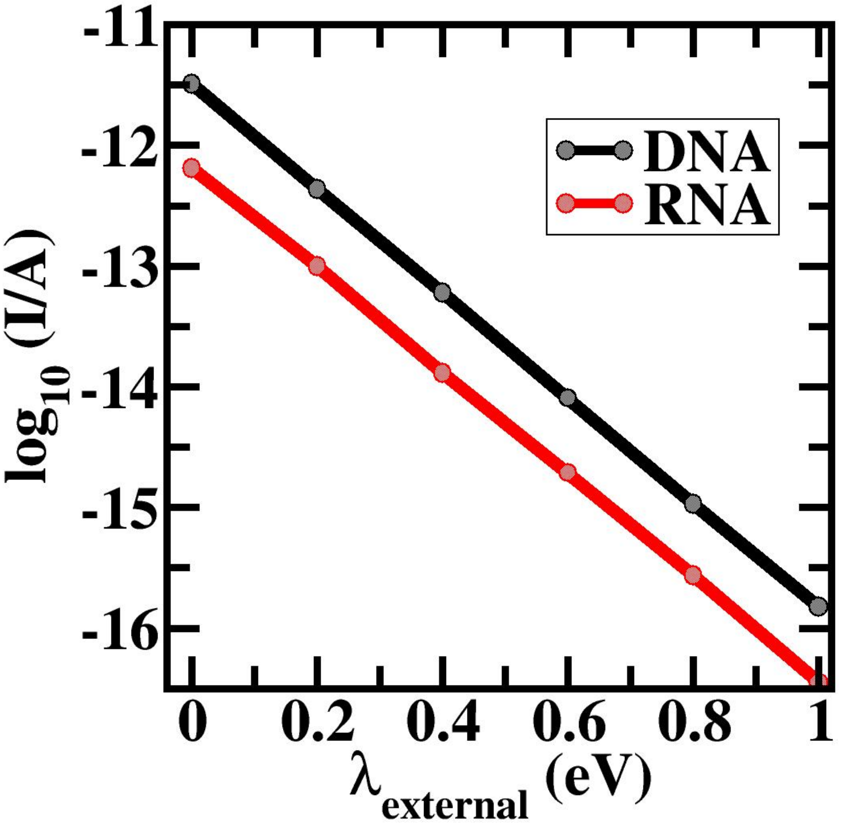

FIG. S8: Variation of current of 12 bp dsDNA (d-(CGCGAATTCGCG)) and dsRNA (d-(CGCGAAUUCGCG)) at an applied potential bias of 1 V with outersphere reorganization energy.

Ionization Energies and Electron Affinities of DNA base pairs

Table **??** lists the ionization energies and electron affinities of DNA and RNA nucleobases.

TABLE SII: Table comparing the ionization energies and electron affinities of DNA and RNA nucleobases

Base	Ionization Energy (eV)	Electron Affinity (eV)
A	6.15	-0.93
C	6.51	-1.32
G	5.74	-0.61
T	6.80	-1.42
U	6.51	-1.33

---

* maiti@iisc.ac.in

[1] J. M. Artés, Y. Li, J. Qi, M. Anantram, and J. Hihath, Nature communications **6**, 8870 (2015).

[2] A. Chatterjee and D. G. Vlachos, Journal of computer-aided materials design **14**, 253 (2007).

[3] V. Rühle, A. Lukyanov, F. May, M. Schrader, T. Vehoff, J. Kirkpatrick, B. Baumeier, and D. Andrienko, Journal of chemical theory and computation **7**, 3335 (2011).

[4] G. I. Livshits, A. Stern, D. Rotem, N. Borovok, G. Eidelshtein, A. Migliore, E. Penzo, S. J. Wind, R. Di Felice, S. S. Skourtis, *et al.*, Nature nanotechnology **9**, 1040 (2014).